Building and Environment 44 (2009) 1850–1863

Contents lists available at ScienceDirect

Building and Environment

journal homepage: www.elsevier.com/locate/buildenv

Predictive control techniques for energy and indoor environmental quality management in buildings

D. Kolokotsa [a,*], A. Pouliezos [b], G. Stavrakakis [c], C. Lazos [c]

[a] Technological Educational Institute of Crete, Department of Natural Resources and Environment, 3, Romanou str., 73133, Hania, Crete, Greece
[b] Technical University of Crete, Department of Production Engineering and Management, University Campus, Kounoupidiana, 73100 Hania, Greece
[c] Technical University of Crete, Department of Electronics and Computer Engineering, University Campus, Kounoupidiana, 73100 Hania, Greece

ARTICLE INFO

Article history:
Received 20 October 2008
Received in revised form
12 December 2008
Accepted 15 December 2008

Keywords:
Energy management systems
Predictive control
Bilinear model
Indoor environmental quality

ABSTRACT

The aim of the present paper is to present a model-based predictive controller, combined with a Building Energy Management System (BEMS). The overall system predicts the indoor environmental conditions of a specific building and selects the most appropriate actions so as to reach the set points and contribute to the indoor environmental quality by minimizing energy costs. The controller is tested using a BEMS installation in Hania, Crete, Greece.

1. Introduction

During the last decades the contribution of Building Energy Management Systems (BEMS) to energy efficiency, improvement of the indoor comfort and environmental quality during a building's operational phase is well recognized. Advanced control techniques based on artificial intelligence (neural networks, fuzzy logic, genetic algorithms, etc.) and distributed control networks offer numerous benefits towards that direction [1–5].

Building energy management and online control systems are reactive to the climatic conditions, building operation and occupancy interventions. Predictive control in conjunction with BEMS on the other hand uses a model to estimate and predict the optimum control strategy to be implemented [6]. While the online control systems can react only to the actual building conditions [7], a model-based predictive control can move forward in time to predict the buildings' reaction to alternative control schemes. Therefore different control scenarios can be evaluated based on suitable objective functions, and create a control state space that corresponds to a building's performance space [8].

A model can be either a "black box" or a "physical" model. In the "black box" or non-physical model approaches, self-learning algorithms, reinforced learning [9] or neural networks [10] are some of the methodologies found in the literature. The benefits of the mentioned approaches are low computational time and the fact that they do not require any specific building modeling expertise, while their limitations are (i) the fact that neural networks require reliable training data that may not be available and (ii) self-learning algorithms cannot move beyond the limits of their experience. When physical models are utilized, the expert has the opportunity to understand the cause-and-effect relationship between the various building components, the control strategies and the climatic conditions. The physical models approach can use stochastic mathematical models [11] or simulation-assisted predictive control [12]. Some physical models though require high computational skills and effort.

In the present work a bilinear model-based predictive control is utilized in conjunction with BEMS, so as to achieve optimum indoor environmental conditions while minimizing energy costs. The bilinear modeling procedure is selected as it is the simplest extension of linear modeling and offers simplicity in the prediction algorithms' calculation procedure. The paper is organized in six sections. Section 2 includes a short description of a building and the installed BEMS. Section 3 incorporates the bilinear model analysis and the identification procedure. Section 4 analyses the predictive control strategy, while Section 5 presents shortly the graphical environment of the predictive control scheme. The experimental analysis including comparison between real and simulated measurements and discussion is presented in Section 6. Finally,

* Corresponding author. Tel.: +30 28210 23017, +30 28210 37209; fax: +30 28210 23003.
E-mail address: kolokotsa@chania.teicrete.gr (D. Kolokotsa).

0360-1323/$ – see front matter
doi:10.1016/j.buildenv.2008.12.007

Section 7 accumulates the conclusions and discusses issues for future research and development.

2. The building energy management system

2.1. Description of the building

The BEMS in which the predictive control scheme is tested, is installed in the Industrial Control Laboratory of the Department of Production and Management Engineering of the Technical University of Crete at Hania, Crete, Greece (35°N latitude). The climatic conditions, i.e., air temperature, humidity and solar radiation on a horizontal surface, of Hania region extracted by METEONORM are illustrated in Fig. 1. The laboratory has 125 m^2 area with almost 3.5 m height, thus 437.5 m^3 volume (see Fig. 2). The building's characteristics including envelope and building services are tabulated in Table 1.

The heating and cooling system is a 30 kW air conditioning system with a cooling power of almost 44 W (38,400 kcal/h). The air conditioning system before the BEMS installation was controlled manually.

The electric lighting in the laboratory uses 94 fluorescent lamps of 58 W and 8 lamps of 18 W.

2.2. The energy management system

The energy management system interconnection is performed using the European Installation Bus-KNX protocol and tools, and is based on a small-scale application presented by the authors' previous work [13]. The monitoring system consists of four sensors for the indoor environment and an outdoor weather station as tabulated in Table 2. The installed actuators are presented in Table 3.

All monitoring and control devices are connected to the European Installation Bus-KNX either directly or by using specific I/O modules (Fig. 3).

3. Predictive control techniques

3.1. Description of the control system

The block diagram of the control system is depicted in Fig. 4 where A represents the actuators and P is the overall BEMS installation. If k is defined as the sample time of BEMS operation then $x(k)$ is the state vector, $y(k)$ is the BEMS' measurements vector,

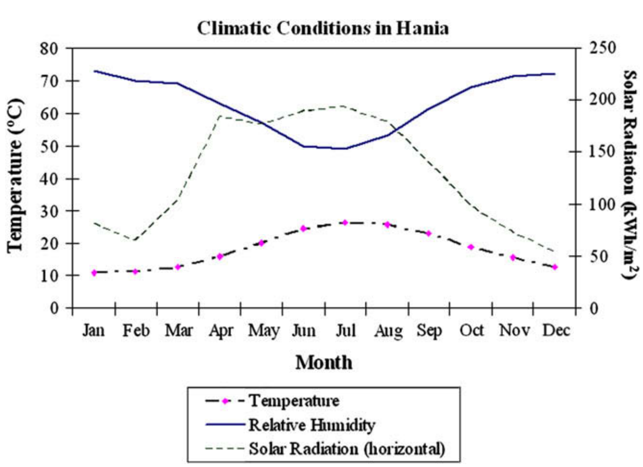

Fig. 1. The climatic conditions in Hania, Crete, Greece.

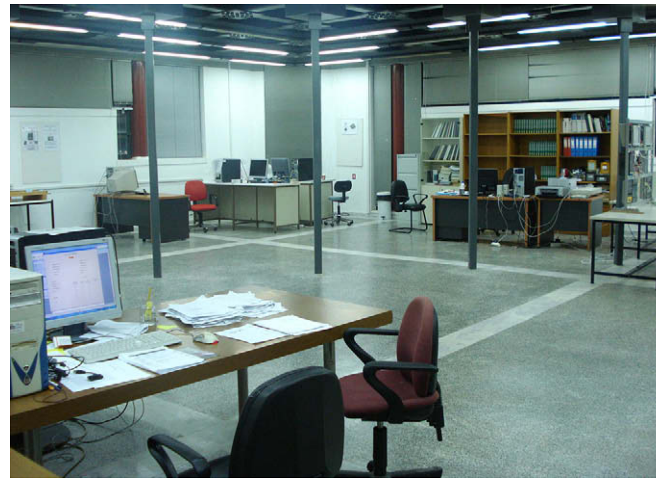

Fig. 2. The laboratory of Department of Production Engineering and Management.

$n(k)$ is the unknown noise for the measurements vector, $u(k)$ the control vector, $d(k)$ the disturbances vector (casual gains, door opening, people smoking, etc.) and x_s is the set-point vector.

The system is then governed by the following equations:

- Nonlinear state equation: $x(k+1) = f(x(k), u(k), d(k))$.
- Measurements with noise: $y(k) = x(k) + n(k)$.
- Controller's output: $u(k) = g(x_s, y(k))$.

More specifically the state vector is:

$$x(k) = [\mathrm{CO}_{2\mathrm{in}}(k) \quad \mathrm{RH}_{\mathrm{in}}(k) \quad T_{\mathrm{in}}(k) \quad E_{\mathrm{in}}(k) \quad \vdots$$
$$\mathrm{CO}_{2\mathrm{out}}(k)\mathrm{RH}_{\mathrm{out}}(k)T_{\mathrm{out}}(k)E_{\mathrm{out}}(k)]^T = \left[x_{\mathrm{in}}^T(k) \quad x_{\mathrm{out}}^T(k)\right]^T \tag{1}$$

where $\mathrm{CO}_{2\mathrm{in}}(k)$ is the indoor CO_2 concentration (in ppm), $\mathrm{RH}_{\mathrm{in}}(k)$ is the indoor relative humidity (%), $T_{\mathrm{in}}(k)$ is the indoor temperature (°C), $E_{\mathrm{in}}(k)$ is the indoor illuminance (lx), $\mathrm{CO}_{2\mathrm{out}}(k)$ is the atmospheric CO_2 concentration (ppm), $\mathrm{RH}_{\mathrm{out}}(k)$ is the outdoor relative humidity (%), $T_{\mathrm{out}}(k)$ is the outdoor temperature (°C) and $E_{\mathrm{out}}(k)$ is the outdoor illuminance (lx).

The control vector is

$$u(k) = [W(k) \quad L(k) \quad S(k) \quad AC(k)]^T \tag{2}$$

where S is shading output (0: fully closed, 1: fully opened, linear output), W is window opening output ((0: fully closed, 1: fully

Table 1
The building's characteristics.

Layer[a]	Material	Depth (m)
Building's envelope characteristics		
External walls		
1	Plaster board	0.013
2	Concrete block	0.035
3	Plaster board	0.013
Floor/roof		
1	Concrete slab	0.030
Door		
1	Iron	0.035
Windows: single glazed iron framed		
1	Glass	0.003
Building services		
Air conditioning		Split type
Electric lighting		Fluorescent lamps

[a] From internal layer to external.

Table 2
The sensors of the BEMS.

Parameter	Manufacturer	Range	Resolution
Indoor illuminance	Siemens 5WG1 252-4AB02 KNX/EIB	200 to 1900 lx	7.68 lx
Indoor Temperature	Siemens 5WG1 256-4AB01	−25 to 70 °C	0.5 °C
Indoor air quality (CO_2 and TVOC)	Siemens QPA63.2	0 to 2000 ppm	20 ppm
Relative humidity	Siemens QFA2000	0 to 100%	1%
Weather station 5WG1 257-3AB11	Raining detection sensor	1: Precipitation 0: No precipitation	
	Luminance sensor	0 to 40,000 lx	156.24 lx
	Outdoor temperature sensor	−20 εως +40 °C.	0.24 °C
	Wind speed sensor	0 to 35 m/s	0.27 m/s

opened, linear output)), AC is heating or cooling output (−1: cooling, +1: heating, 0:closed, Pulse Width Modulation (PWM)), L, lighting output (%) (0: lights OFF, 100: lights ON, linear output).

The desired values (set point) state vector is

$$x_s = \begin{bmatrix} CO_{2sp} & RH_{sp} & T_{sp} & E_{sp} \end{bmatrix}^T \tag{3}$$

where CO_{2sp} is CO_2 concentration set point, RH_{sp} is relative humidity set point, T_{sp} is temperature set point and E_{sp} is illuminance set point.

3.2. Model development and model identification

3.2.1. Model description

The buildings' environmental variables are modeled using a bilinear approach [14] described by the following equation:

$$\begin{aligned} x_p(k+1) = {} & x_p(k) + \lambda_1 \cdot f_1(u(k), x_p(k), d(k)) + \cdots \\ & + \lambda_m \cdot f_m(u(k), x_p(k), d(k)) \end{aligned} \tag{4}$$

where $\lambda_i = \lambda_1 \ldots \lambda_m$ are the coefficients that correspond to the specific building operation and are estimated during the system's identification procedure [15].

The bilinear model takes different forms for each environmental variable as analyzed below.

3.2.1.1. Carbon dioxide concentration. The indoor carbon dioxide concentration at time $(k+1)$ is a linear function of the indoor carbon dioxide concentration at time (k), the window opening at time (k) and the outdoor concentration as described in the following equation:

$$CO_{2in}(k+1) = CO_{2in}(k) + a_1 W(k)[CO_{2out}(k) - CO_{2in}(k)] \tag{5}$$

where a_1 is a constant to be estimated during model identification procedure.

3.2.1.2. Relative humidity. Similarly the indoor relative humidity at time $(k+1)$ is expressed as a linear function of the indoor relative humidity, the window opening, the air conditioning output and finally the outdoor relative humidity RH_{out} at time (k).

$$RH_{in}(k+1) = RH_{in}(k) + \beta_1 W(k)[RH_{out}(k) - RH_{in}(k)] + \beta_2 AC(k) \tag{6}$$

where β_1 and β_2 are parameters to be estimated during model identification procedure.

3.2.1.3. Indoor temperature. The indoor temperature at time $(k+1)$ is a linear function of the parameters comprising the following equation, i.e., the indoor temperature, the window opening position, the outdoor temperature and the air conditioning output at time (k).

$$\begin{aligned} T_{in}(k+1) = {} & T_{in}(k) + \gamma_1 W(k)[T_{out}(k) - T_{in}(k)] + \gamma_2 AC(k) \\ & + \gamma_3 [T_{out}(k) - T_{in}(k)] \end{aligned} \tag{7}$$

where γ_1, γ_2 and γ_3 are parameters to be estimated during model identification procedure.

3.2.1.4. Lighting level. Finally, the indoor illuminance at time $(k+1)$ is a function of outdoor illuminance, shading output and lighting output at time (k).

$$E_{in}(k+1) = \delta_1 S(k) E_{out}(k) + \delta_2 L(k) + \delta_3 E_{out}(k) \tag{8}$$

where δ_1, δ_2 and δ_3 are parameters to be estimated during model identification procedure.

Therefore, based on Eqs. (5)–(8), the system is described by the bilinear model of the form:

$$\begin{aligned} x(k+1) = {} & \begin{bmatrix} 1 & 0 & 0 & 0 & 0 & 0 & 0 & 0 \\ 0 & 1 & 0 & 0 & 0 & 0 & 0 & 0 \\ 0 & 0 & 1-\gamma_3 & 0 & 0 & 0 & \gamma_3 & 0 \\ 0 & 0 & 0 & 0 & 0 & 0 & 0 & \delta_3 \\ 0 & 0 & 0 & 0 & \phi_1(k) & 0 & 0 & 0 \\ 0 & 0 & 0 & 0 & 0 & \phi_2(k) & 0 & 0 \\ 0 & 0 & 0 & 0 & 0 & 0 & \phi_3(k) & 0 \\ 0 & 0 & 0 & 0 & 0 & 0 & 0 & \phi_4(k) \end{bmatrix} x(k) \\ & + \begin{bmatrix} -\alpha_1 & 0 & 0 & 0 & \alpha_1 & 0 & 0 & 0 \\ 0 & -\beta_1 & 0 & 0 & 0 & \beta_1 & 0 & 0 \\ 0 & 0 & -\gamma_2 & 0 & 0 & 0 & \gamma_2 & 0 \\ 0 & 0 & 0 & 0 & 0 & 0 & 0 & 0 \\ 0 & 0 & 0 & 0 & 0 & 0 & 0 & 0 \\ 0 & 0 & 0 & 0 & 0 & 0 & 0 & 0 \\ 0 & 0 & 0 & 0 & 0 & 0 & 0 & 0 \\ 0 & 0 & 0 & 0 & 0 & 0 & 0 & 0 \end{bmatrix} x(k)W(k) \\ & + \begin{bmatrix} 0 & 0 & 0 & 0 & 0 & 0 & 0 & 0 \\ 0 & 0 & 0 & 0 & 0 & 0 & 0 & 0 \\ 0 & 0 & 0 & 0 & 0 & 0 & 0 & 0 \\ 0 & 0 & 0 & 0 & 0 & 0 & 0 & \delta_1 \\ 0 & 0 & 0 & 0 & 0 & 0 & 0 & 0 \\ 0 & 0 & 0 & 0 & 0 & 0 & 0 & 0 \\ 0 & 0 & 0 & 0 & 0 & 0 & 0 & 0 \\ 0 & 0 & 0 & 0 & 0 & 0 & 0 & 0 \end{bmatrix} x(k)S(k) + 0 \cdot x(k)L(k) \\ & + 0 \cdot x(k)AC(k) + \begin{bmatrix} 0 & 0 & 0 & 0 \\ 0 & 0 & 0 & \beta_2 \\ 0 & 0 & 0 & \gamma_1 \\ 0 & \delta_2 & 0 & 0 \\ 0 & 0 & 0 & 0 \\ 0 & 0 & 0 & 0 \\ 0 & 0 & 0 & 0 \\ 0 & 0 & 0 & 0 \end{bmatrix} u(k) \end{aligned} \tag{9}$$

or

$$x(k+1) = Ax(k) + \sum_{j=1}^{4} G_j x(k) u_j(k) + Bu(k) \tag{10}$$

The outdoor variables (measured or assumed constant) are modeled by dummy equations of the form

$$x_{i+4}(k+1) = \varphi_i(k) \times x_{i+4}(k) \tag{11}$$

for $i = 1, \ldots, 4$.

Table 3
The actuators of the BEMS.

Output	Device	Type	No. of actuators required
Lighting control	Electronic ballasts for the fluorescent lamps of 18 W and 58 W	DALI	49
	Digital Addressable Lighting Interface	DALI interface	1
Windows control Shading control	Shutter switch N524 N561	Siemens 5WG1 524-1AB01 0–100%	1 with 4 different outputs
Air conditioning control	Binary output N561	KNX/EIB	1

3.2.2. Model identification

The identification procedure consists of the estimation of the λ_i, parameters of Eq. (1). The methodology used is the standard least squares defined by Eq. (12) or (13):

$$\begin{bmatrix} x_p(2)-x_p(1) \\ x_p(3)-x_p(2) \\ \vdots \\ x_p(n-1)-x_p(n-2) \\ x_p(n)-x_p(n-1) \end{bmatrix} = \begin{bmatrix} f_1(u(1),x_p(1)) & \cdots & f_m(u(1),x_p(1)) \\ f_1(u(2),x_p(2)) & \cdots & f_m(u(2),x_p(2)) \\ \vdots & \ddots & \vdots \\ f_1(u(n-2),x_p(n-2)) & \cdots & f_m(u(n-2),x_p(n-2)) \\ f_1(u(n-1),x_p(n-1)) & \cdots & f_m(u(n-1),x_p(n-1)) \end{bmatrix} \begin{bmatrix} \lambda_1 \\ \vdots \\ \lambda_m \end{bmatrix} \tag{12}$$

or

$$x = F\lambda \tag{13}$$

where $x_p(k)$ are the predicted values. The least squares estimator is defined by

$$\hat{\lambda} = \left(F^T F\right)^{-1} F^T x \tag{14}$$

Based on Eq. (14) the next time step value $x_p(k+1)$ is predicted given the present time step values $x_p(k)$, $u(k)$ by

$$x_p(k+1) = x_p(k) + \hat{\lambda}_1 f_1(u(k),x_p(k)) + \cdots + \hat{\lambda}_m f_m(u(k),x_p(k)) \tag{15}$$

The least squares estimation is performed separately for each actuator by putting the BEMS in continuous operation mode for at least 48 h with sample time equal to 2 min. During the estimation and identification process the actuators' position is moving gradually from its minimum to its maximum value with a 10% step in order to cover the overall range in the first 24 h. This procedure is repeated for the next 24 h. At the end, each actuator is interrelated to the four environmental variables.

The least squares estimation is also tested under various climatic conditions providing similar outputs.

In the following paragraphs the model identification procedure is presented for each environmental variable.

3.2.2.1. Carbon dioxide concentration. Before estimating the relevant constants in the CO_2 equation the outdoor carbon dioxide concentration must be estimated. Due to lack of an extra CO_2 sensor, the indoor CO_2 sensor was positioned outdoors for a 10-day period. During this period the outdoor CO_2 measurements fluctuated between 475 and 520 ppm with an average almost equal to 497 ppm. Consequently the outdoor CO_2 concentration can be considered constant and equal to the average value. The model extracted is presented by Eq. (15). The predicted values follow closely the real ones as depicted in Fig. 5.

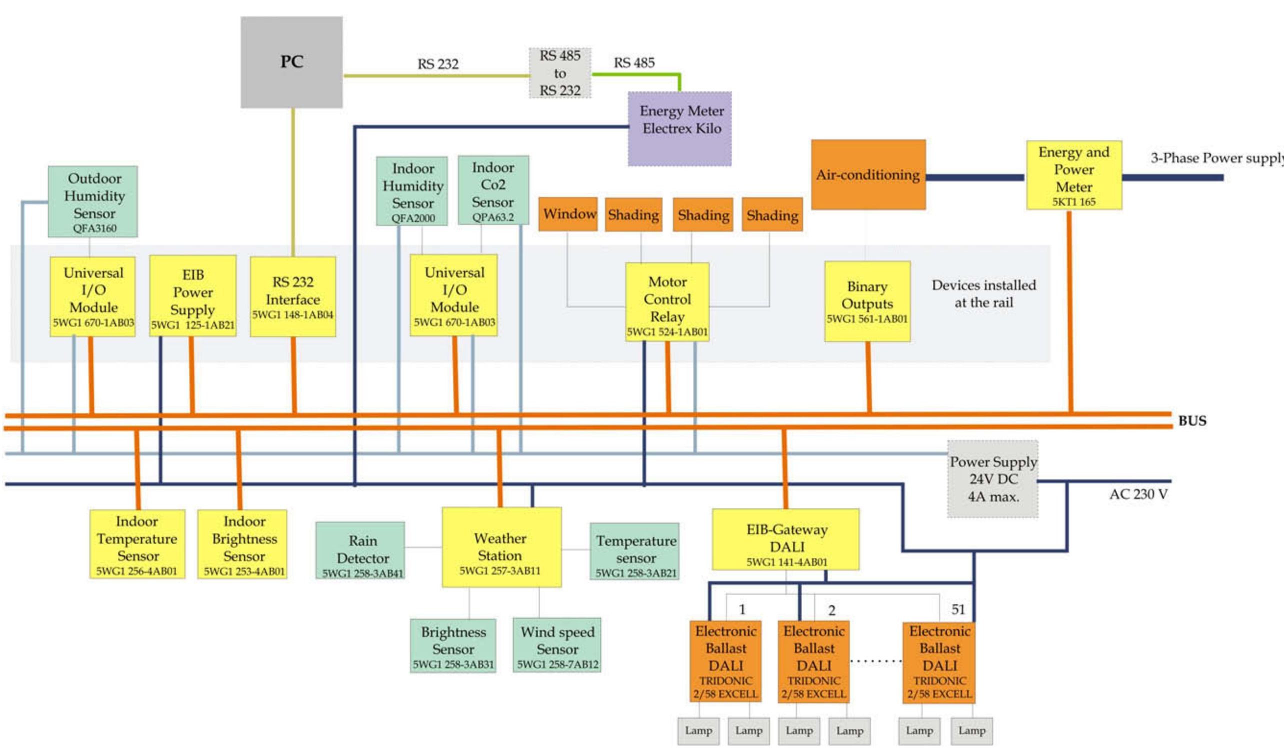

Fig. 3. The energy management system installation layout.

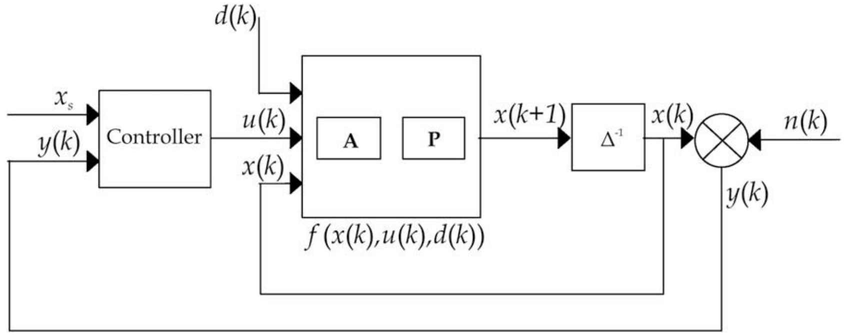

Fig. 4. The control system's block diagram.

The R^2 is equal to 0.466, while the root mean square error (RMSE) is equal to 4.658 ppm.

$$CO_{2in}(k+1) = CO_{2in}(k) + 0.215W(k)[497 - CO_{2in}(k)] \tag{16}$$

3.2.2.2. Lighting level. The illuminance model is described by Eq. (16). The model identification is performed separately for the electric lighting regulation and shading regulation. The model identification for electric lighting regulation and for shading regulation only is depicted in Fig. 6 and Fig. 7, respectively. The R^2 between the real and predicted measurements is equal to 0.9026, while the RMSE is between 60 and 67 lx.

$$E_{in}(k+1) = 0.0033 \cdot S(k) \cdot E_{out}(k) + 4.05L(k) + 0.008 \cdot E_{out}(k) \tag{17}$$

3.2.2.3. Indoor temperature. The indoor temperature model is described for the specific building characteristics by the following equation:

$$T_{in}(k+1) = T_{in}(k) + 0.0029 \cdot W(k)[T_{out}(k) - T_{in}(k)] + 0.0756 \cdot AC(k) + 0.0039[T_{out}(k) - T_{in}(k)] \tag{18}$$

Fig. 8 illustrates the real and predicted temperature values for closed windows and air conditioning system operation only, while Fig. 9 depicts the real and predicted temperature for closed air conditioning systems and windows regulation only. The R^2 between the real and predicted measurements is equal to 0.9981, while the RMSE is 0.18 °C.

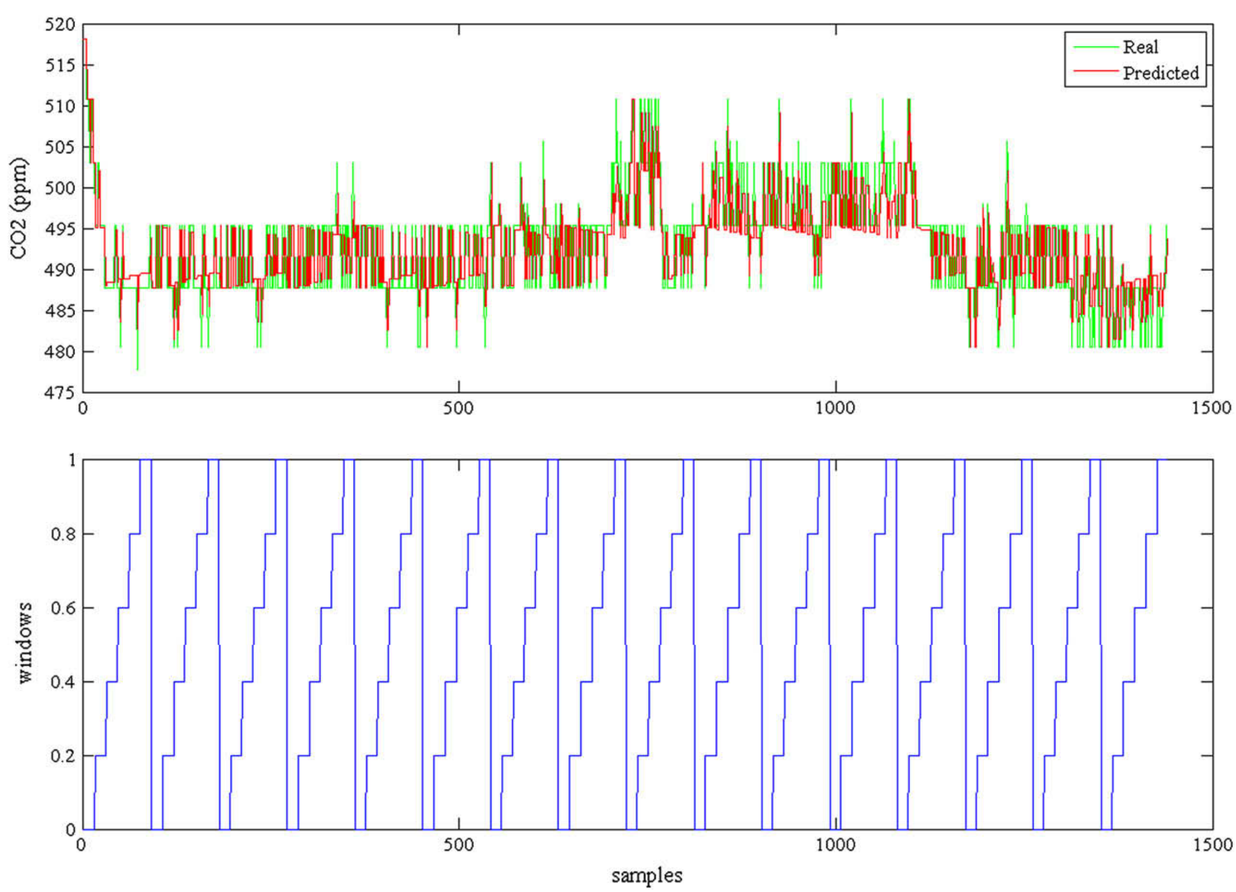

Fig. 5. The carbon dioxide model.

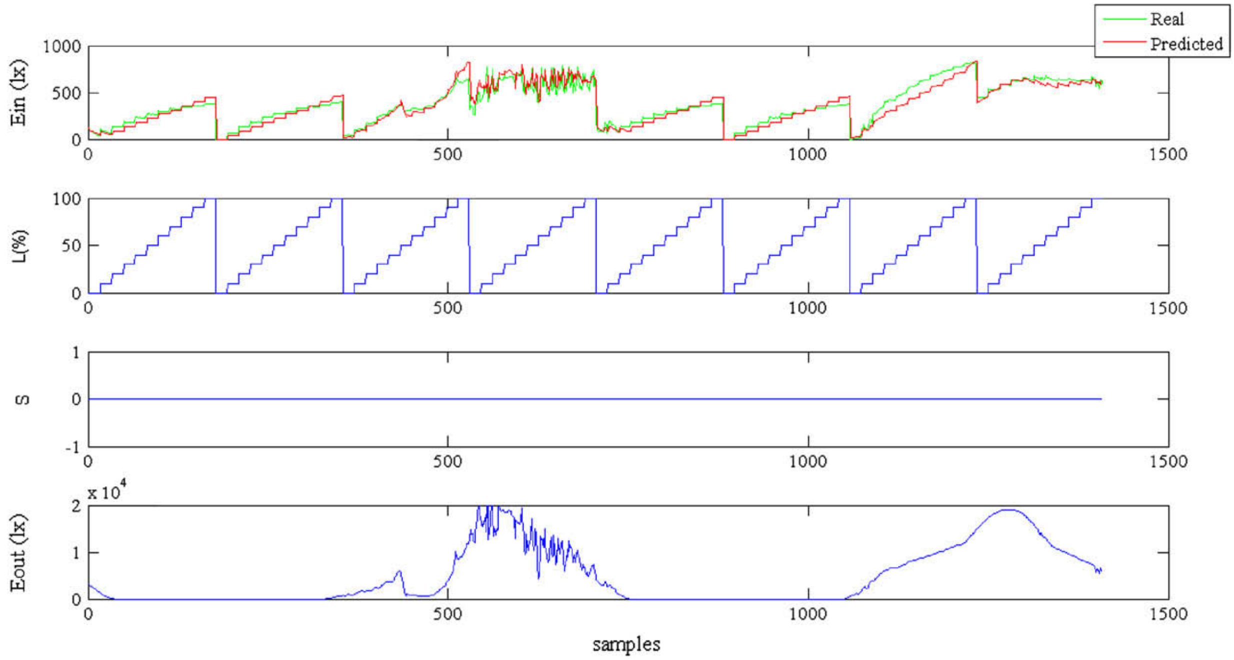

Fig. 6. The lighting model with closed shading devices.

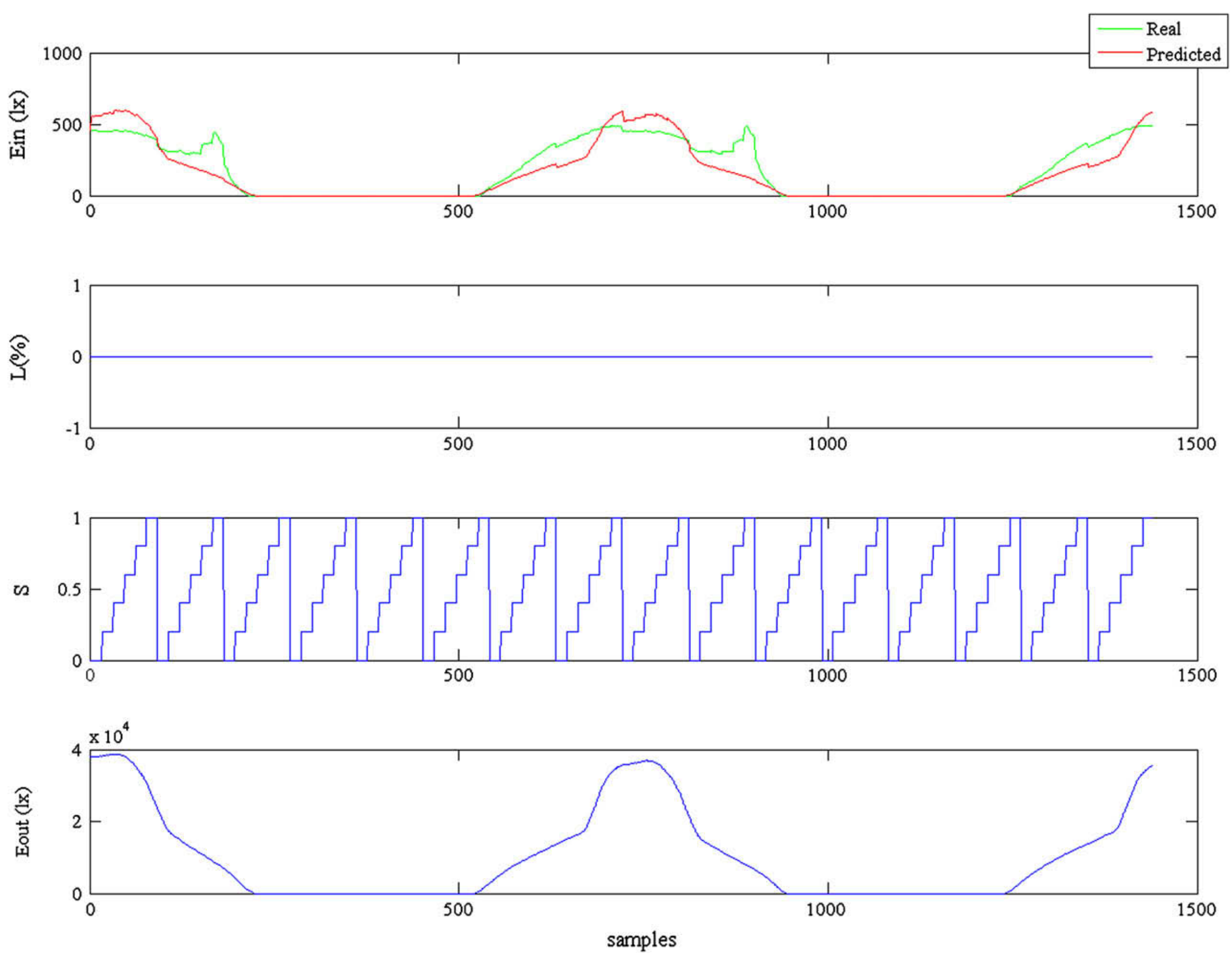

Fig. 7. The lighting model with closed electric lighting.

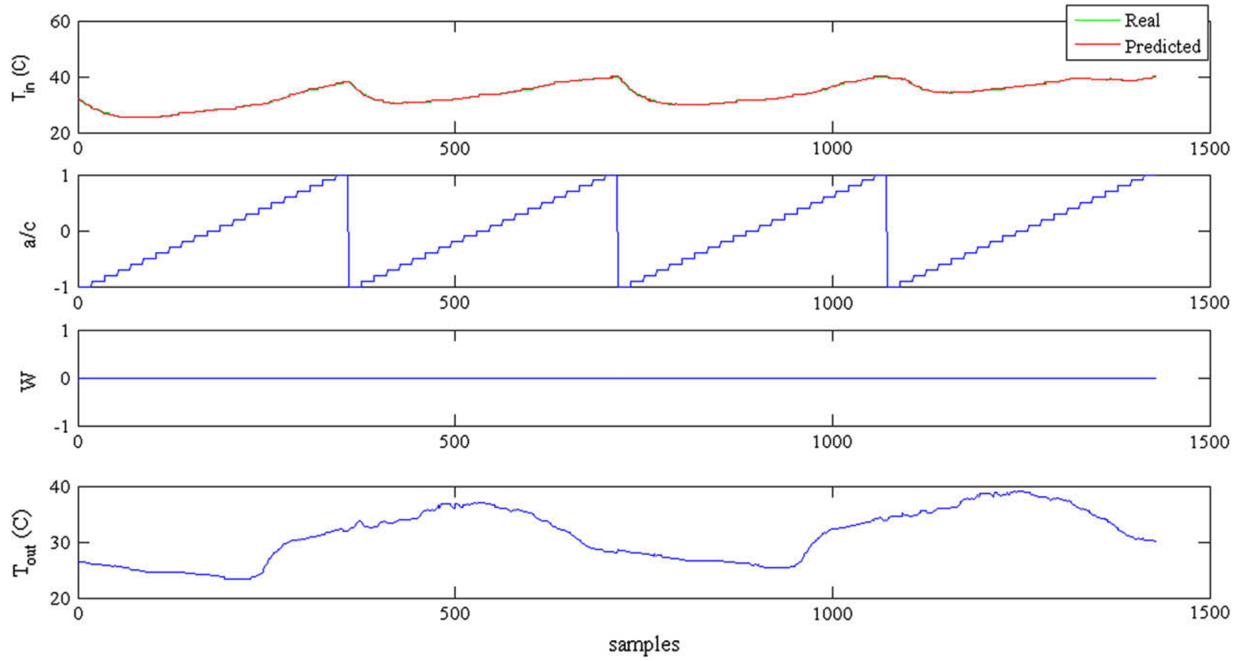

Fig. 8. The temperature model with closed windows.

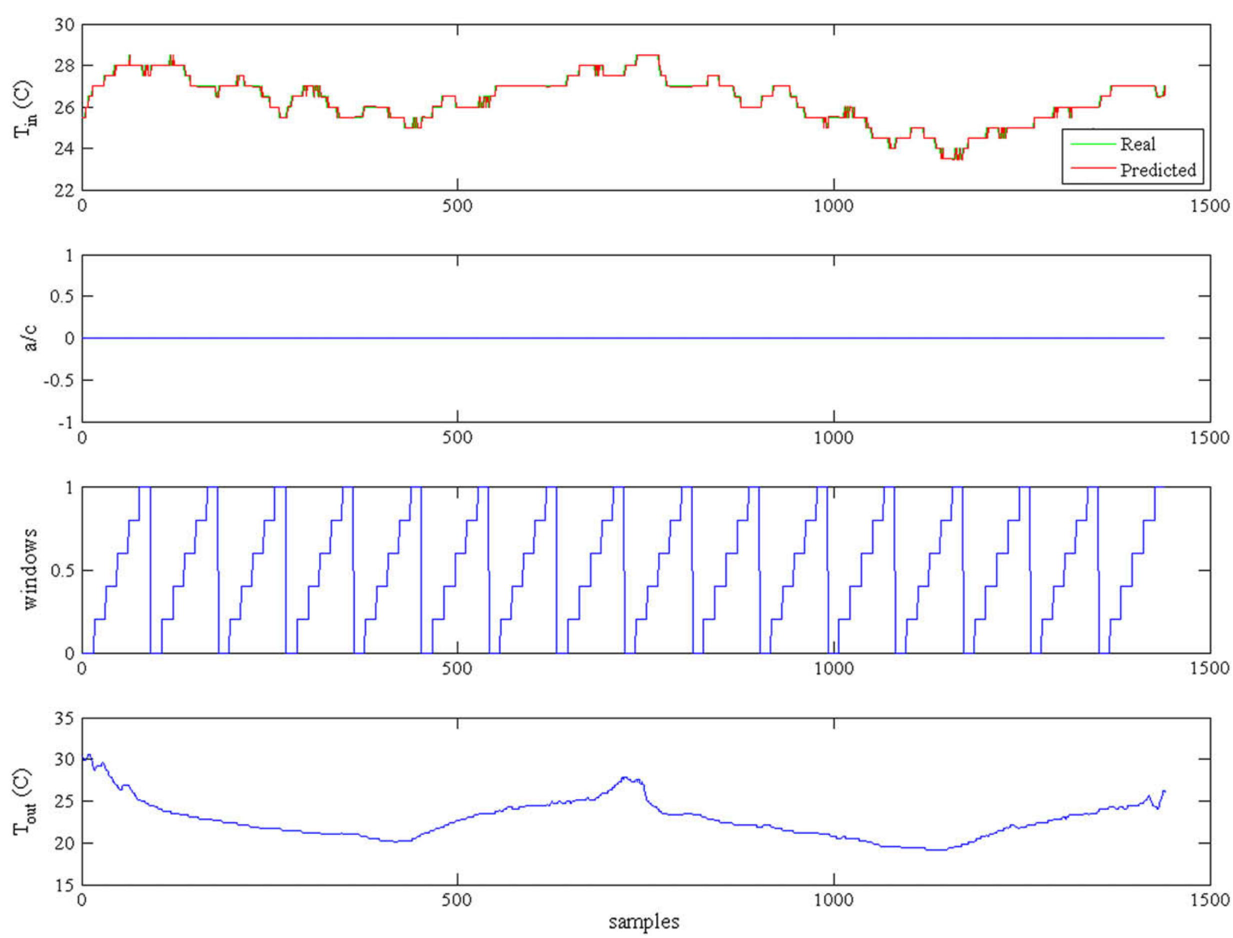

Fig. 9. The temperature model with closed air conditioning system.

3.2.2.4. Relative humidity. The humidity identification model is represented by Eq. (18) and the relevant graphs are Fig. 10 and Fig. 11, respectively.

$$\mathrm{RH_{in}}(k+1) = \mathrm{RH_{in}}(k) + 0.0077\cdot W(k)[RH_{\mathrm{out}}(k) - Hum_{\mathrm{in}}(k)] + 0.0747\cdot \mathrm{AC}(k) \tag{19}$$

The R^2 between the real and predicted measurements is equal to 0.9947 and the RMSE is 0.39.

In all graphs we can see that the predicted values follow closely the real values. Therefore the identification procedure for the bilinear model can be considered quite accurate.

4. Controller design and development

The controller is designed to minimize a performance index $J(k)$, which aims to keep the environmental variables as close as possible to the defined set points x_s and simultaneously minimize the energy consumption. $J(k)$ is defined as

$$J(k) = \|x_{\mathrm{in}}(k+1) - x_s\|_Q^2 + \|u(k)\|_R^2 \tag{20}$$

where Q and R are weight matrices corresponding to the proximity of the set points and the actuators' electric energy cost, respectively [14].

The $J(k)$ index can be estimated after a series of N sample times where each sample time is set equal to 2 min. Therefore the objective is to

$$\min_{u\in U} J = \|x_{\mathrm{in}}(k+N) - x_s\|_Q^2 + \|u(k)\|_R^2 \tag{21}$$

The following assumptions are made:

- The control values remain constant for the prediction horizon, $u(k) = u(k+1) = \cdots = u(k+N)$.
- The external disturbances future values are assumed constant and equal to their last measured values, i.e., $x_{\mathrm{out}}(k) = x_{\mathrm{out}}(k+1) = \cdots = x_{\mathrm{out}}(k+N) = \tilde{x}_{\mathrm{out}}(k)$.
- The actuators for the shading devices (S) and window opening (W) do not include "energy costs" and therefore receive zero weight in matrix R.
- The lighting actuator (L) can influence only the state of lighting and consequently can be minimized independently.

As a result the weight matrices are defined as

$$Q = a\cdot \mathrm{diag}[q_1 \quad q_2 \quad q_3 \quad q_4] \tag{22}$$

$$R = (1-a)\cdot \mathrm{diag}[r_1 \quad r_2 \quad r_3 \quad r_4] \tag{23}$$

where a, $q_i = q_1, q_2, q_3, q_4$ and $r_i = r_1, r_2, r_3, r_4$ are selected based on trial and error in order to reflect the differences between the scales of the environmental variables as well as to establish a balance between a variable's value and the corresponding control cost.

Moreover the control space U is discretized to simplify the minimization procedure. The discrete space is the following:

$U_{d,\mathrm{W}} = \{0, 0.1, 0.2, \ldots, 1\}$ for window opening output;
$U_{d,\mathrm{L}} = \{0, 10, 20, \ldots, 100\}$ for electric lighting output;
$U_{d,\mathrm{S}} = \{0, 0.1, 0.2, \ldots, 1\}$ for shading output; and
$U_{d,\mathrm{AC}} = \{-1, -0.9, \ldots 0, 0.1, 0.2, \ldots, 1\}$ for air conditioning output.

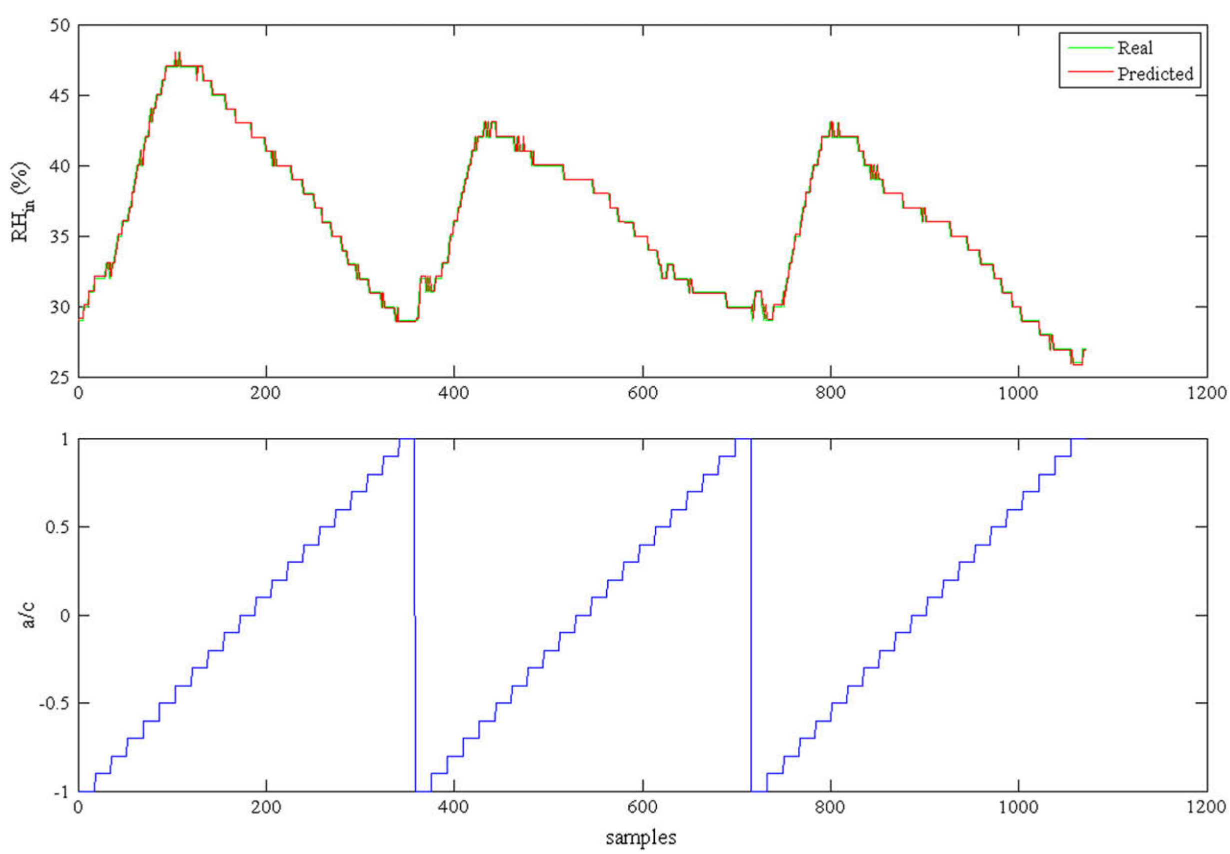

Fig. 10. The humidity model with closed windows.

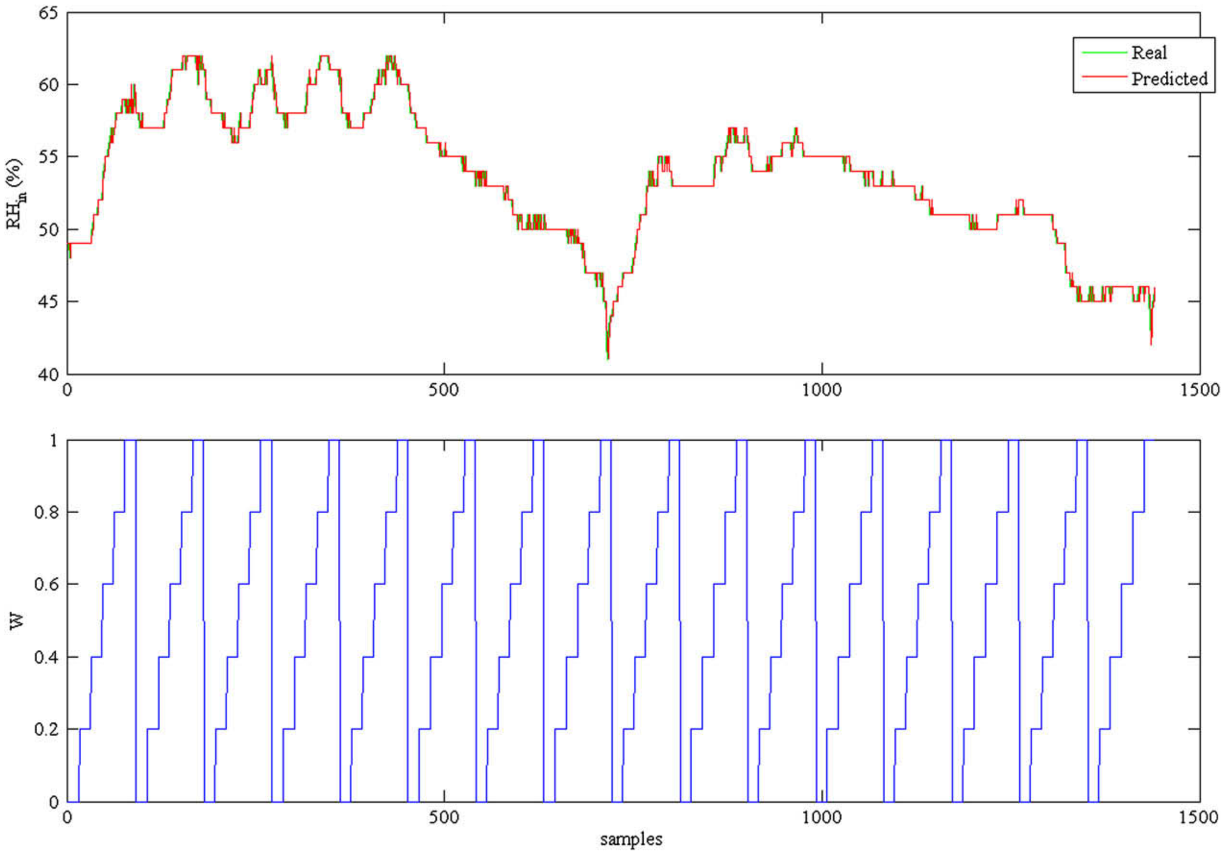

Fig. 11. The humidity model with closed air conditioning system.

4.1. Controller design parameters

4.1.1. Set points

The set points for the environmental variables are based on the international literature and are summarized in Table 4.

More specifically for the indoor air quality, CO_2 concentration levels above 1000 ppm create unhealthy environment for the occupants based on standards and guidelines [16,17]. Moreover the National Institute for Occupational Safety and Health (NIOSH) indicates that CO_2 concentration levels above 1000 ppm indicate poor ventilation rates [18]. Following the above analysis the set point is set equal to 600 ppm with a 100 ppm dead band.

Based on the ASHRAE standard 55.2004 [19] for thermal comfort, the set point for relative humidity is equal to 50% with a 10% dead band.

The indoor temperature set point depends upon the climatic conditions and has a seasonal variation based on EN 15251 [20] (see Table 4).

The indoor illuminance level according to the standard 1926.56 of the Occupational Safety & Health Administration (OSHA) should be at least 300 lx [21]. In the laboratory a 350 lx set point is selected.

Table 4
The environmental parameters set points.

Environmental parameter	Set points	
Indoor temperature	*WINTER* T_{sp} 21 °C	*SUMMER* T_{sp} 26 °C
Relative humidity	50%	
CO_2 concentration	600 ppm	
Illuminance	350 lx	

Therefore the set-point vector is

$$x_s = \begin{bmatrix} 600 & 50 & T_{sp} & 350 \end{bmatrix} \tag{24}$$

4.1.2. The prediction horizon

After trial and error the prediction horizon is set equal to $N = 5$ samples. This is decided in order not to move away from the present realistic conditions for the external disturbances and also not to limit the prediction margin.

4.1.3. The Q and R weight matrices

As mentioned in the previous sections, the Q matrix refers to the set points' proximity. The weight values are selected in order to achieve normalization between the environmental variables. Normalization is performed by dividing the maximum value from the set-point vector with the set point for each variable.

This leads to

$$w_{CO_2} = 600/600 = 1, w_{RH} = 600/50 = 12, w_{T_{in}} = 600/25 = 24$$

Table 5
The Q matrix weights.

Environmental parameter	Weights
Indoor temperature	$w_{T_{in}} = \left\{ \begin{matrix} 0 & \text{if } 21\,^\circ\text{C} \le T_{in} < 26\,^\circ\text{C} \\ 20 & \text{if } T_{in} \ge 26\,^\circ\text{C or } T_{in} < 21\,^\circ\text{C} \end{matrix} \right\}$
Relative humidity	$w_{RH} = \left\{ \begin{matrix} 0 & \text{if } 40\% \le RH_{in} \le 60\% \\ 12 & \text{if } RH_{in} < 40\% \text{ or } RH_{in} > 60\% \end{matrix} \right\}$
CO_2 concentration	$w_{CO_2} = \left\{ \begin{matrix} 0 & \text{if } CO_{2,in} < 600\text{ ppm} \\ 1 & \text{if } CO_{2,in} \ge 600\text{ ppm} \end{matrix} \right\} 0$
Illuminance	1

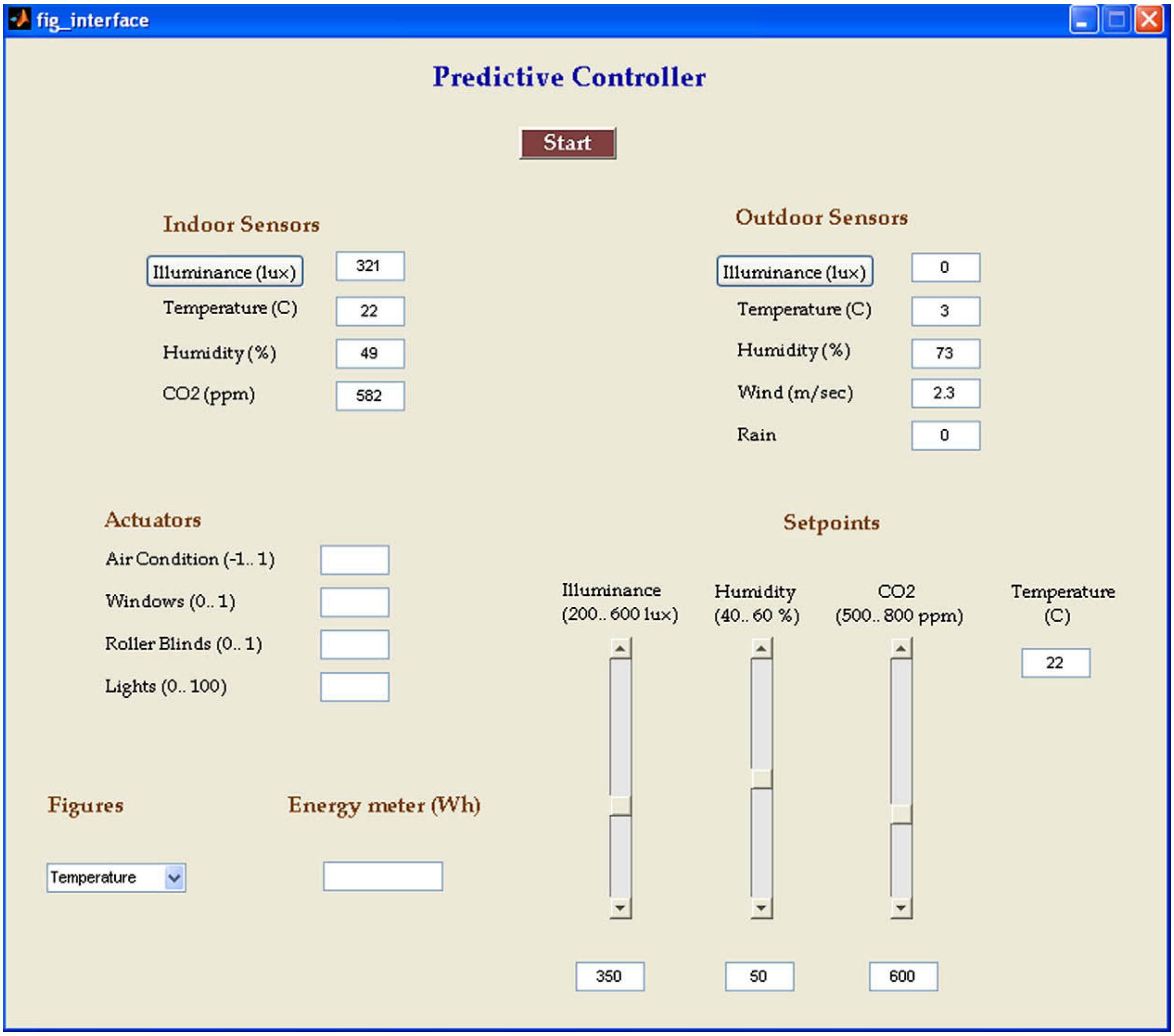

Fig. 12. The user interface.

Indoor temperature weight is evaluated by dividing by 25 °C, which represents the average outdoor temperature conditions. The lighting levels are minimized independently and the weight selected is equal to 1,

$$W_E = 1$$

For the external disturbances we put

$$w_{CO_2,\text{ext}} = 0, w_{RH,\text{ext}} = 0, w_{T,\text{ext}} = 0, w_{E,\text{ext}} = 0$$

The weights are set according to the variables' values measured as tabulated in Table 5.

For instance if the carbon dioxide concentration is lower than 600 ppm then the system should not act in order to reach the set point and therefore the Q matrix weight is set equal to 0. The same applies if the measured relative humidity is between 40 and 60% and if the indoor temperature is between 21 and 26 °C.

Therefore the Q matrix is set as

$$Q = a \cdot \text{diag}[q_1 \quad q_2 \quad q_3 \quad q_4] = a \cdot \text{diag}[w_{CO_2} \quad w_{RH} \quad w_{T_{in}} \quad 1] \tag{25}$$

The R matrix expresses the electricity cost for the actuators' operation. The windows and shading operation cost is almost zero compared to the air conditioning operation cost. Consequently, $r_1 = r_3 = 0$ for the R matrix. The weighting for the air conditioning system is set equal to 8 to express its large contribution to the energy cost. The weighting for the lights is equal to 1. Following the above, R is expressed as follows:

$$\begin{aligned} R &= (1-a) \cdot \text{diag}[r_1 \quad r_2 \quad r_3 \quad r_4] \\ &= (1-a) \cdot \text{diag}[0 \quad 1 \quad 0 \quad 8] \end{aligned} \tag{26}$$

Finally we select $a = 0.5$ since the two minimization matrices Q and R are equally important.

4.1.4. *Sample time*

Although in the initial design phase the sample time was 2 min, the final sample time selected is 10 min to avoid fatigue especially for the air conditioning system due to continuous opening and closing.

5. The system–user interface

The role of building users is very critical for the system's performance nowadays where the shifting towards passive sustainable buildings instead of tight controlled air conditioned

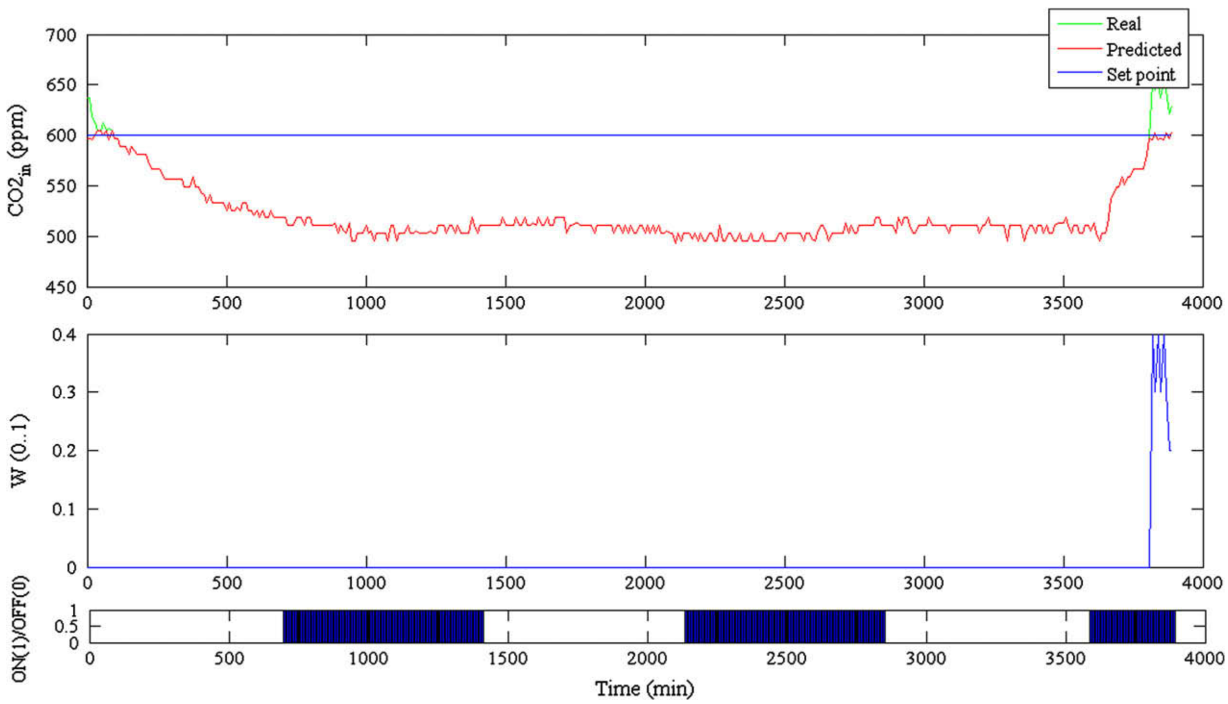

Fig. 13. Carbon dioxide measurements.

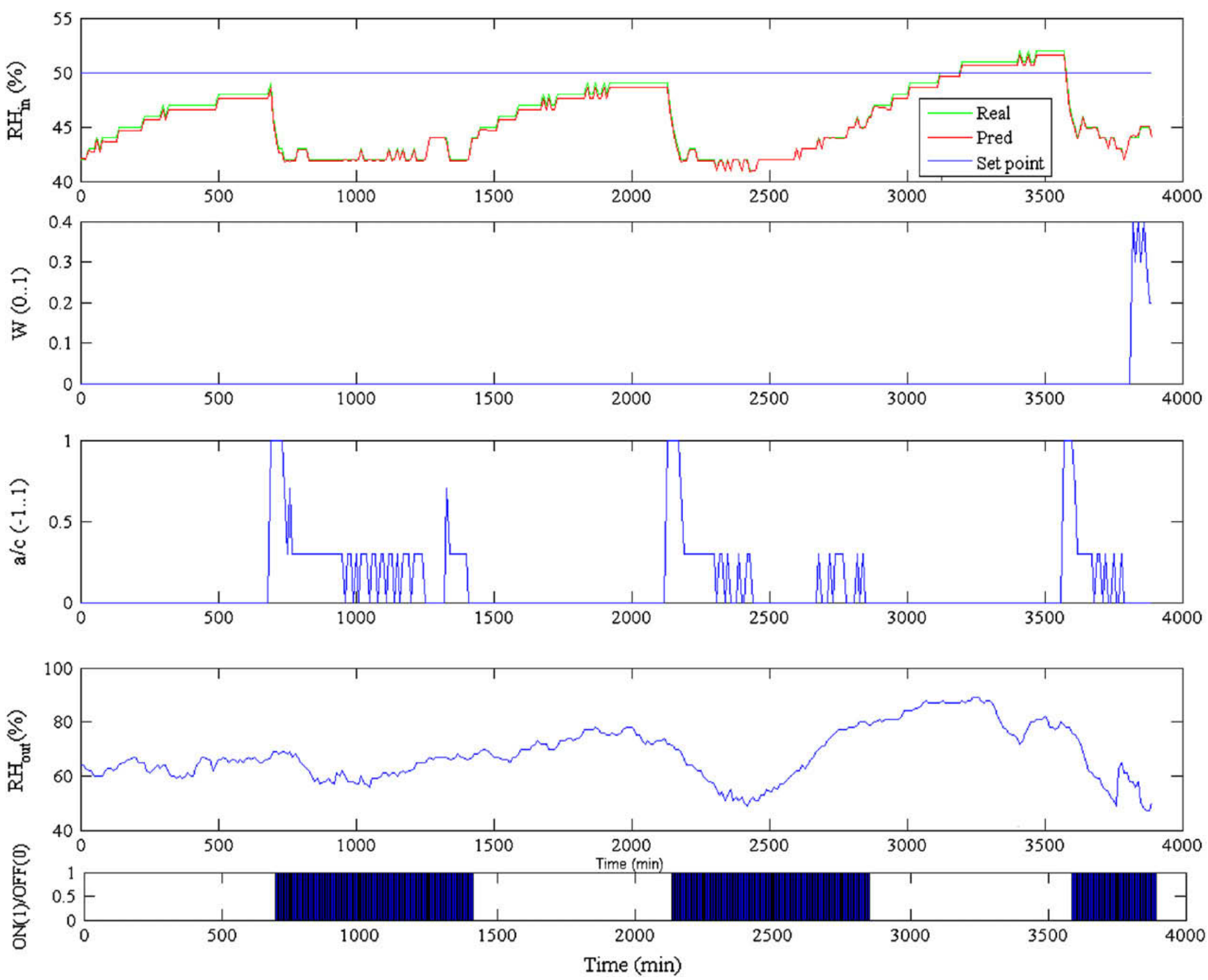

Fig. 14. Relative humidity measurements.

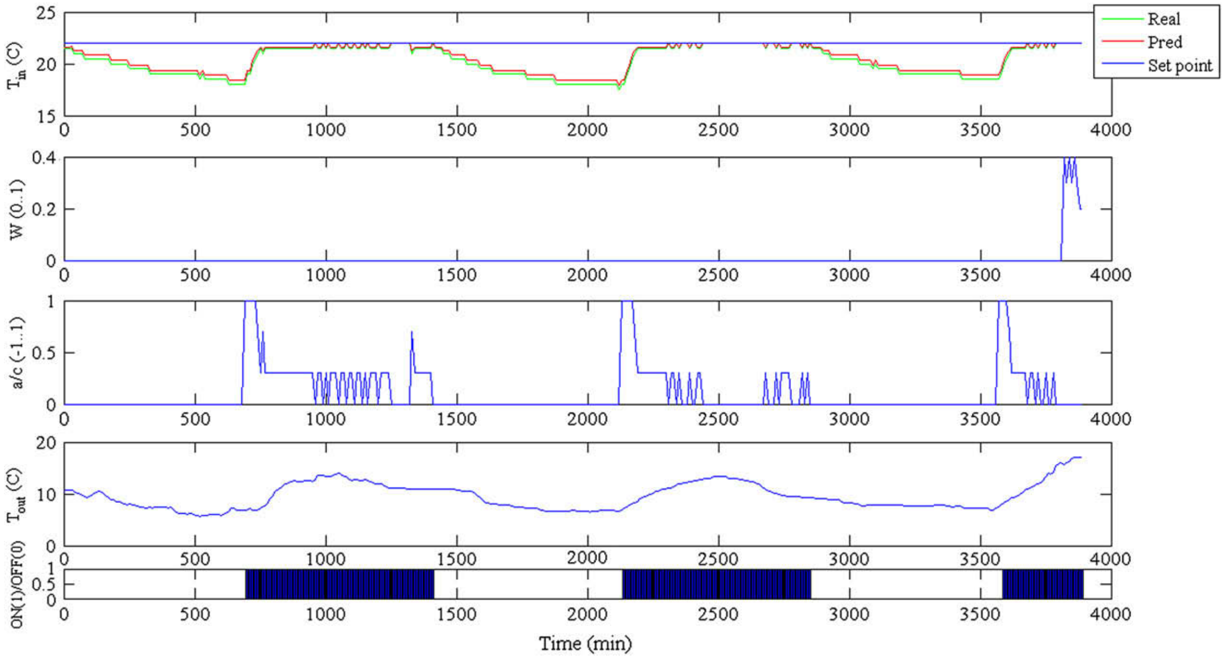

Fig. 15. Temperature measurements.

buildings requires more active users with higher comfort expectations [22]. Moreover users demand control of their environment. Therefore a graphical environment and a system–user interface application are considered necessary.

Fig. 12 illustrates the graphical environment of the proposed predictive building energy management system. The graphical environment includes (a) the start/stop button; (b) the sensors' current values; (c) the actuators position; (d) the set-point bars and finally the button to extract 24 h graphs.

The interface is used by the user to perform the following operations:

⇛ To set the system on or off.

⇛ To change the set points according to users' comfort requirements by using the roller bar.

⇛ To monitor the indoor environmental conditions.

⇛ To change the actuators' position manually when needed (for example in case of a presentation).

The graphical user interface provides the capability to the user to interact with BEMS. Also the user can overcome the BEMS operation according to his/her needs.

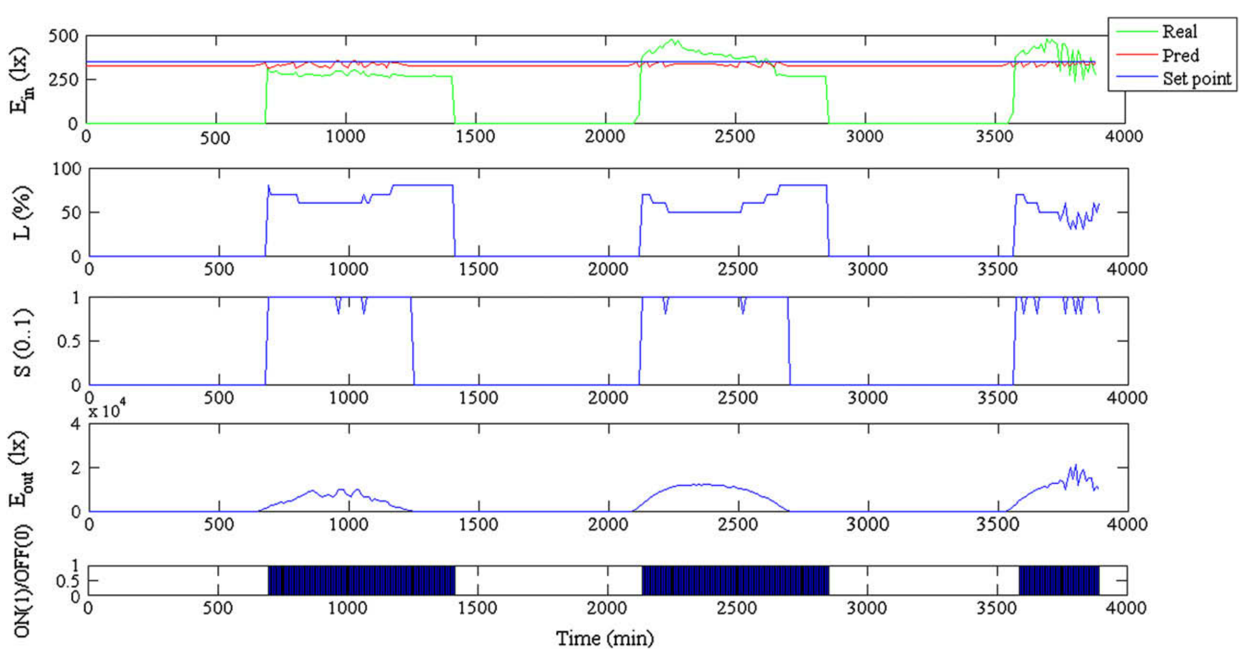

Fig. 16. Illuminance measurements.

6. Experimental results analysis and discussion

The overall system was tested for various periods. The sample time measurements were 10 min to coincide with the operational period of the predictive controller. The measurements were stored in specific files and were also used for the state vector of the controller (Eq. (1)). Although the results are discrete, they are presented in a continuous format for visualization purposes.

The experimental analysis presented below is performed between 11 January 2008 and 14 January 2008 for an overall period of 3900 min or 65 h. It should be noted that a time programming is also applied to set the system off each night between 20:00 and 8:00.

The carbon dioxide measurements while the predictive controller was operating are presented in Fig. 13. The upper graph includes the CO_2 set point, the real measurements of the sensors and the predicted values by the bilinear model. The lower graph indicates the actuators' (window) position. In the bottom of each graph an on/off diagram illustrates the time periods that the system was operating (using the START/STOP button of the graphical user interface). As we can see in Fig. 13 the real measurements coincide with the predicted ones while there is no presence in the lab. When students enter the lab the systems react immediately and open the windows to reduce the carbon dioxide concentration.

For the humidity measurements (Fig. 14) four graphs are illustrated. The first upper graph incorporates the indoor measurements, the predicted values by the bilinear model and the set point. The 40–60% window is defined by the dashed lines. The second graph illustrates the window positions while the third one represents the air conditioning operation positions. Finally the fourth graph indicates the outdoor relative humidity measurements. The relative humidity is always between the respected margins as illustrated in Fig. 14.

When the system is in operation the indoor temperature is within the acceptable margins. The windows are kept closed due to the external climatic conditions and are opened for ventilation purposes only (Fig. 15).

Temperature measurements are also presented in four graphs (Fig. 15) with the same logic as for the relative humidity measurements. Finally the lighting levels are depicted in Fig. 16. The four graphs of Fig. 16 correspond to the illuminance measurements, shading outputs, lighting outputs and outdoor lighting levels, respectively.

Finally the indoor illuminance is kept close to the desired set point with fluctuations that attributed to the external illuminance and are not considered important for the visual comfort.

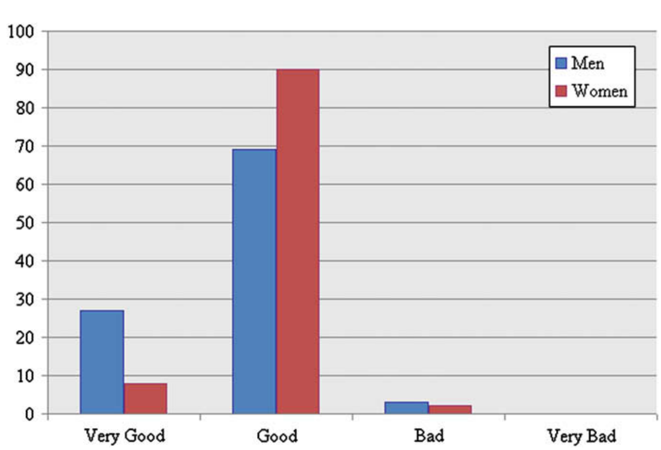

Fig. 17. Users' comfort assessment.

In all graphs the x-axis represents the time period of the system's operation. In each figure there is a graph at the bottom which indicates the periods that the system is operating ((ON(1) – blue color) or not (OFF(0))).

The BEMS is operating continuously since December 2007 in order to test it under different climatic conditions. The model identification procedure does not show any seasonal variation. Therefore the models extracted can be used under any climatic conditions.

Another significant issue is the occupants' perception of comfort while the BEMS is in operation. The indoor comfort conditions were assessed during summer 2008 using a questionnaire. The users' perception on indoor thermal comfort is illustrated in Fig. 17 where the majority of the students found the indoor environmental conditions quite satisfactory.

7. Conclusions and future prospects

The present BEMS supported by a model-based predictive controller follows the initial design specifications and objectives. The system's response to the environmental variables' fluctuations is fast and stable.

Considerable variations between the predicted and the real values are observed for the carbon dioxide concentration. This can be attributed to the fact that the window opening is small in comparison with to the building's volume and cannot contribute significantly to regulate the people's contribution and disturbances satisfactorily. The CO_2 concentration though is kept close to the requested set point.

Finally the controller's performance is quite satisfactory and selects the optimum solutions based on the energy consumption and the set-point proximity by satisfying the performance index J. It remains to future investigations to expand the performance index J to include indoor comfort requirements and improve the predictive control algorithm using different prediction techniques.

References

[1] Kolokotsa D, Niachou K, Geros V, Kalaitzakis K, Stavrakakis G, Santamouris M. Implementation of an integrated indoor environment and energy management system. Energy and Buildings 2005;37(1):93–9.
[2] Kolokotsa D. Artificial intelligence in buildings: a review on the application of fuzzy logic. Advances in Building Energy Research 2007;1(1):29–54.
[3] Kalogirou S. Artificial neural networks in energy applications in buildings. International Journal of Low Carbon Technologies 2006;1(3):201–16.
[4] Dounis AI, Santamouris MJ, Lefas CC, Manolakis DE. Thermal comfort degradation by a visual comfort fuzzy-reasoning machine under natural ventilation. Applied Energy 1994;48(2):115–30.
[5] Dounis AI, Santamouris MJ, Lefas CC, Argiriou A. Design of a fuzzy set environment comfort system. Energy and Buildings 1995;22(1):81–7.
[6] Clarke JA, Conner S, Fujii G, Geros V, Jóhannesson G, Johnstone CM, Karatasou S, Kim J, Santamouris M, Strachan PA. The role of simulation in support of Internet-based energy services. Energy and Buildings 2004;36(8):837–46.
[7] Doukas H, Patlitzianas KD, Iatropoulos K, Psarras J. Intelligent building energy management system using rule sets. Building and Environment 2007;42(10):3562–9.
[8] Mahdavi A, Pröglhöf C. A model-based approach to natural ventilation. Building and Environment 2008;43(4):620–7.
[9] Dalamagidis K, Kolokotsa D, Kalaitzakis K, Stavrakakis GS. Reinforcement learning for energy conservation and comfort in buildings. Building and Environment 2007;42(7):2686–98.
[10] Karatasou S, Santamouris M, Geros V. Modelling and predicting building's energy use with artificial neural networks: methods and results. Energy and Buildings 2006;38(8):949–58.
[11] Loveday DL, Virk GS. Artificial intelligence for buildings. Applied Energy 1992;41(3):201–21.
[12] Clarke JA, Cockroft J, Conner S, Hand JW, Kelly NJ, Moore R, O'Brien T, Strachan P. Simulation-assisted control in building energy management systems. Energy and Buildings 2002;34(9):933–40.
[13] Kolokotsa D, Saridakis G, Pouliezos A, Stavrakakis GS. Design and installation of an advanced EIB™ fuzzy indoor comfort controller using Matlab™. Energy and Buildings 2006;38(9):1084–92.

[14] Ekman M. Modeling and control of bilinear systems, applications to the activated sludge process. Dissertation for PhD in automatic control, Uppsala University; 2005.
[15] Kolokotsa D, Pouliezos A, Stavrakakis G. Sensor fault detection in building energy management systems. In: Proceedings of the 5th international conference on technology and automation ICTA '05, 15–16 October 2005, Thessaloniki, Greece, p. 282–287.
[16] World Health Organization (WHO). Air quality guidelines for Europe. In: European series. 2nd ed., No. 91. Regional Publications; 2000.
[17] ASHRAE 62.1-2004. Ventilation for acceptable indoor air quality. USA: American Society of Heating, Refrigerating, Air-Conditioning Engineers; 2004.
[18] Spengler JD, Samet JM, McCarthy JF. Indoor air quality handbook. US: McGraw-Hill; 2000.
[19] ASHRAE Standard 55-2004. Thermal environmental condition for human occupancy. USA: American Society of Heating, Refrigerating, Air-Conditioning Engineers; 2004.
[20] EN15251:2006. Indoor environmental input parameters for design and assessment of energy performance of buildings – addressing indoor air quality, thermal environment, lighting and acoustics. CEN; 2006.
[21] U.S. Department of Labor. Safety and health regulations for construction, subpart D – occupational health and environmental controls paragraph. 1926.56, illumination. U.S. Department of Labor; 1997.
[22] Hoes P, Hensen JLM, Loomans MGLC, de Vries B, Bourgeois D. User behavior in whole building simulation. Energy and Buildings 2009;41(3):295–302.